

Research Article

Synthesis, Physicochemical Characterization, and Cytotoxic Activity of *p*-Methoxyphenyl and *p*-Fluorophenyl Maleanilic Acid Ligands and Their Corresponding Organometallic Chelates of Chromium Group

Khlood R. Oraby,¹ M. A. Zayed,² Fatma S. M. Hassan,¹ and Adila E. Mohamed¹

¹Chemistry Department, Faculty of Science, Aswan University, 81528 Aswan, Egypt

²Chemistry Department, Faculty of Science, Cairo University, 12613 Giza, Egypt

Address correspondence to Khlood R. Oraby, kholoud_oraby@sci.aswu.edu.eg

Received 9 November 2019; Revised 16 January 2020; Accepted 28 January 2020

Copyright © 2020 Khlood R. Oraby et al. This is an open access article distributed under the terms of the Creative Commons Attribution License, which permits unrestricted use, distribution, and reproduction in any medium, provided the original work is properly cited.

Abstract A new *p*-methoxyphenyl (ML) and *p*-fluorophenyl (FL) maleanilic acid bidentate ligands were green synthesized by a solvent-free reaction of equimolar amounts of aniline derivatives (4-methoxyaniline or 4-fluoroaniline) with maleic anhydride. Additionally, some mixed ligand organometallic chelates of Cr(0), Mo(0), and W(0) carbonyls were synthesized by the addition of the prepared ligand (L) as a primary ligand to the hexacarbonyl metals, in which carbonyl groups are secondary ligands in a 1:1 molar ratio. The structures of the novel chelates were characterized by elemental analyses, FT-IR, EI-MS, ¹H-NMR spectroscopy, and thermal analyses. FL maleanilic acid free ligand and its chromium complex were screened for antitumor activity in vitro against cell lines of HCT-116 (human colon carcinoma), hepG-2 (human hepatocellular carcinoma), and MCF-7 (human breast carcinoma). The results obtained referred to a high antitumor activity of both FL novel ligand and its chromium organometallic chelates.

Keywords *p*-methoxyphenyl and *p*-fluorophenyl maleanilic acid ligands; organometallic chelates; spectroscopic and thermal analyses; antitumor screening

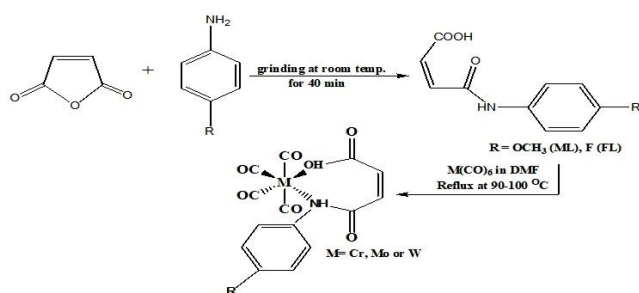
1. Introduction

Numerous compounds containing metal and carbon monoxide have been prepared for a long time. Compounds having at least one bond between carbon and metal are known as organometallic compounds. Metal carbonyls are the transition metal complexes of carbon monoxide containing metal-carbon bonds. Lone pairs of electrons are available on both carbon and oxygen atoms of carbon monoxide ligand. However, as the carbon atoms donate electrons to the metal, these complexes are named as carbonyls [1]. Metal carbonyls are most of the time nonpolar and electrically neutral compounds and demonstrate physical properties of organic compounds. The general formula of metal carbonyls is $M_x(CO)_y$. These complexes may be homoleptic, that is containing only CO ligands, such as nickel carbonyl ($Ni(CO)_4$), but more commonly metal carbonyls contain a mix of ligands such as $Re(CO)_3(2,2'$ -bipyridine)Cl. Metal carbonyls are highly toxic compounds because of their tendency to carbonylate hemoglobin to give

carboxyhemoglobin, which will not bind O_2 . They react vigorously with oxygen and oxidizing substances, and some ignite spontaneously. Metal carbonyls include solubility in only organic solvents but have poor solubility with water and volatile solid or liquid appearance at room temperature. Nevertheless, metal carbonyls serve as precursors for the preparation of other organometallic complexes [2].

On the other side, the chemistry of the amide group ($-CONH_2$) containing ligands is of great importance because it offers two potential binding atoms (the carboxylate oxygen and the amide nitrogen atom) as two coordination sites. This is in addition to their analytical, industrial, and pharmacological properties [3,4,5]. Maleanilic acid and its derivatives are one of the most important amide groups containing ligands; they are endowed with various types of biological activities. They are antitubercular agents; in addition to other pharmacological uses [6,7,8]. Furthermore, these compounds act as fungicides, herbicides, and plant growth regulators [9,10,11,12]. In organometallic chemistry, a number of complexes were reported with amide group ligands, which exhibit diverse coordinating behavior with different metal ions [13,14,15,16]. This feature returns to the fact that the maleanilic acid ligands coordinate to metals through the nitrogen of secondary amide and the oxygen of the carboxylate groups [5].

The above facts motivated us to prepare two derivatives of maleanilic acid ligands, *p*-methoxyphenyl (ML) and *p*-fluorophenyl (FL) maleanilic acid free ligands. Hence, we synthesized novel mixed ligand complexes of general formula $[M(CO)_4L]$ (where $M = Cr, Mo$ or W ; and $L = ML$ or FL) by the reaction of ML or FL free ligands with the metal atom in the form of hexacarbonyl metals $M(CO)_6$ (where $M = Cr, Mo$ or W). The molecular structures of the synthesized mixed ligand complexes were characterized and studied by elemental analyses, Fourier-transform infrared spectroscopy (FT-IR), electron ionization mass



Scheme 1: Synthetic route of maleanilic acid derivatives ML and FL as free ligands and their novel complexes.

spectroscopy (EI-MS), proton nuclear magnetic resonance ($^1\text{H-NMR}$) spectroscopy, and thermal analyses. Also, we are interested in the study of the biological and antitumor activity of FL maleanilic acid and its chromium complex in vitro against cell lines of MCF-7 (human breast carcinoma), HCT-116 (human colon carcinoma), and hepG-2 (human hepatocellular carcinoma).

2. Experimental

2.1. Materials and reagents

All chemicals used in the present study are of analytical reagent grade and of the highest purity available. They include maleic anhydride, 4-fluoroaniline, 4-methoxyaniline, $\text{Cr}(\text{CO})_6$, $\text{Mo}(\text{CO})_6$, and $\text{W}(\text{CO})_6$. They are purchased from Sigma Aldrich (MO, USA). This is in addition to absolute ethanol, dimethylformamide (DMF), and dimethylsulfoxide (DMSO) which are purchased from Alpha Aesar and used without further purification.

2.2. Instrumentation

Weights measurement was performed using sensitive analytical balance (0.0001 g, SCALTEC; Germany). Stirring and heating were performed using a thermostatic hotplate magnetic stirrer (VELP; Europe). A melting-point apparatus (GallenKamp; Germany) was used to investigate the melting points. Elemental microanalysis of the separated solid compounds for C, H, and N was performed in the Microanalytical Centre, Cairo University. The infrared spectra were measured using a Perkin Elmer FT-IR type 1650 spectrophotometer in the wavenumber region $4000\text{--}400\text{ cm}^{-1}$ as KBr disks. $^1\text{H-NMR}$ spectroscopy was recorded on a Bruker DPX 400 spectrometer (300.068787 MHz); DMSO was used as the internal reference solvent. The EI-MS measurements were obtained using Shimadzu GC-MS-Qp 1000 PX quadruple mass spectrometer. The thermal analyses of the novel compounds were made using a conventional thermal analyzer (Shimadzu system of 30 series TG-50). These instruments were calibrated using indium metal as a thermally stable material. The reproducibility of the instrument reading was determined by repeating each experiment more than twice.

2.3. Synthesis of free ligands and complexes

2.3.1. Synthesis of free ligands

ML was prepared by mixing both of *p*-methoxyaniline (0.1 mol, 12.32 g) and maleic anhydride (0.1 mol, 9.8 g) in a 1:1 molar ratio and grinding them at room temperature for 40 min using an agate mortar [17]. During crunching, a nice greenish-yellow product appeared. The product was recrystallized from absolute ethanol and dried under vacuum over P_2O_5 to calculate the yield (92%). All the above steps were repeated for FL maleanilic acid with a yield of about 88%. The synthesis of maleanilic acid derivatives ML and FL as ligands are schematically represented in Scheme 1.

2.3.2. General procedures for the synthesis of the novel complexes of maleanilic acid derivatives

Chromium complex of ML ligand was prepared by Cooper et al. modified method [18] in which the prepared ML maleanilic acid ligand (0.11 g, 0.5 mmol) was dissolved in the least amount of DMF, then added to $\text{Cr}(\text{CO})_6$ (0.11 g, 0.5 mmol). The volume of the reaction mixture solution was completed to 20 mL using DMF solvent. It was stirred for 40 min under reflux at $90\text{--}100\text{ }^\circ\text{C}$. After refluxing, a dark yellow solution appeared. The collected product was filtered off, washed thoroughly with absolute ethanol, recrystallized from DMF/ethanol mixture and dried under vacuum. All the above steps were repeated for all the selected transition metal complexes 1–6. The synthesis of the novel complexes of maleanilic acid derivatives is schematically represented in Scheme 1.

2.4. Pharmaceutical materials and methods

The cell lines of HCT-116, HepG-2, and MCF-7 cells were obtained from VACSERA Tissue Culture Unit (Giza, Egypt); crystal violet and trypan blue dyes were purchased from Sigma Aldrich. DMSO, fetal bovine serum, DMEM, RPMI-1640, HEPES buffer solution, L-glutamine, gentamycin, and 0.25% trypsin-EDTA were purchased from Lonza (Basel, Switzerland); crystal violet stains were 1%. The cells were propagated in Dulbecco's Modified Eagle's Medium (DMEM) supplemented with 10% heat-inactivated fetal bovine serum, 1% L-glutamine, HEPES buffer, and $50\text{ }\mu\text{g mL}^{-1}$ gentamycin. All cells were maintained at $37\text{ }^\circ\text{C}$ in a humidified atmosphere with 5% CO_2 and were subcultured two times a week. The cells were seeded in 96-well plate at a cell concentration of 1×10^4 cells per well in $100\text{ }\mu\text{L}$ of growth medium. Fresh medium containing different concentrations of the test sample was added after 24 h of seeding. Serial two-fold dilutions of the tested chemical compound were added to confluent cell monolayers dispensed into 96-well, flat-bottomed microtiter plates (Falcon; NJ, USA) using a multichannel pipette. The microtiter plates were incubated at $37\text{ }^\circ\text{C}$ in a humidified incubator with 5% CO_2 for a period of 48 h.

Table 1: Physical measurements and analytical data of ML and FL ligands and their metal complexes 1–6.

No.	Molecular mass/molecular formula	m/z	Yield (%)	Melting point (°C)	Elemental analysis (%) calc. (found)		
					C	H	N
ML	C ₁₁ H ₁₀ O ₄ N	220.21	92	199	59.99 (60.71)	4.58 (5.08)	6.36 (6.41)
FL	C ₁₀ H ₇ O ₃ NF	208.17	88	217	57.69 (57.42)	3.39 (3.85)	6.72 (6.71)
1	[CrC ₁₅ H ₁₁ O ₈ N]	383.33	68	180	47.27 (47.39)	2.70 (2.90)	3.65 (3.14)
2	[MoC ₁₅ H ₁₁ O ₈ N]	428.18	62	< 200 d	42.07 (41.83)	2.58 (3.41)	3.27 (4.08)
3	[WC ₁₅ H ₁₁ O ₈ N]	516.09	91	230	34.93 (34.01)	2.15 (2.2)	2.71 (3.13)
4	[CrC ₁₄ H ₈ O ₇ NF]	373.06	85	200	45.07 (46.06)	2.16 (3.04)	3.75 (2.91)
5	[MoC ₁₄ H ₈ O ₇ NF]	417.01	77	195	40.32 (40.93)	1.93 (2.41)	3.36 (3.50)
6	[WC ₁₄ H ₈ O ₇ NF]	505.03	77	< 260 d	33.29 (34.03)	1.59 (3.08)	2.77 (3.45)

d: decomposed

Three wells were used for each concentration of the test sample. Control cells were incubated without test sample and with or without DMSO. The little percentage of DMSO present in the wells (maximal 0.1%) was found not to affect the experiment. After incubation of the cells for at 37 °C, various concentrations of the sample were added, the incubation was continued for 24 h, and viable cells yield was determined using MTT assay [19,20].

3. Results and discussion

3.1. Characterization of ML and FL ligands and their novel metal complexes

ML and FL ligands were prepared by the method described above (Scheme 1). The structures of the synthesized ligands were established by elemental analyses, FT-IR, EI-MS, ¹H-NMR spectrometry, and thermal analyses. Cr, Mo or W novel complexes of the ML and FL ligands were synthesized in a 1:1 molar ratio (metal:ligand), using the described metal atoms in the form of hexacarbonyl metals M(CO)₆ (Scheme 1). The synthesized metal complexes of the chemical formula of [M(CO)₄L], where M = Cr, Mo or W and L = ML or FL, are microcrystalline in nature and stable at room temperature. They are insoluble in common organic solvents such as chloroform and acetone but they are completely soluble in DMSO and DMF. Unfortunately, we failed to grow the single crystal of metal complexes. Therefore, in order to have a better understanding of the molecular structure, we have performed the elemental analysis, FT-IR, EI-MS, ¹H-NMR spectroscopy, and thermal analyses. Physical measurements and elemental analyses data of the novel complexes 1–6 are given in Table 1. The elemental analyses of the ligands and their complexes reveal good agreement with the proposed structures.

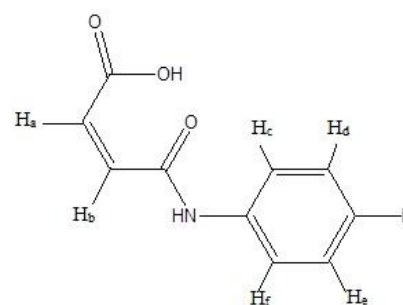


Figure 1: Proposed structure of ligands.

3.2. ¹H-NMR spectra

The ¹H-NMR spectra for ML, FL ligands and their complexes have been recorded in DMSO solvent. The ¹H-NMR spectrum of ML showed that a singlet at δ 3.71 ppm of relative intensity 3H may be attributed to OCH₃ protons. Another singlet at δ 12.88 ppm of relative intensity 1H is observed and may be assigned to OH proton of the carboxylic acid. The amide proton HNCO is observed as a singlet at δ 10.38 ppm. The aromatic protons *ortho* to the methoxy group (H^e, H^d) are observed as a doublet of doublets at δ 7.51–7.58 ppm and another doublet of doublets at δ 7.88–6.92 ppm for the protons which are *ortho* to the amide group (H^c, H^f). The two doublets signals (H^c, H^f) and (H^e, H^d) have the same coupling constant *J* and the same integrated area, indicating the presence of four protons with two couples that are chemically equivalent but not magnetically equivalent [21]. The vinylic protons (H^a, H^b) are observed as a doublet of doublets at δ 6.45–6.44 ppm and δ 6.27–6.30 ppm of relative intensity 1H. The proposed structure of the free ligands is given in Figure 1.

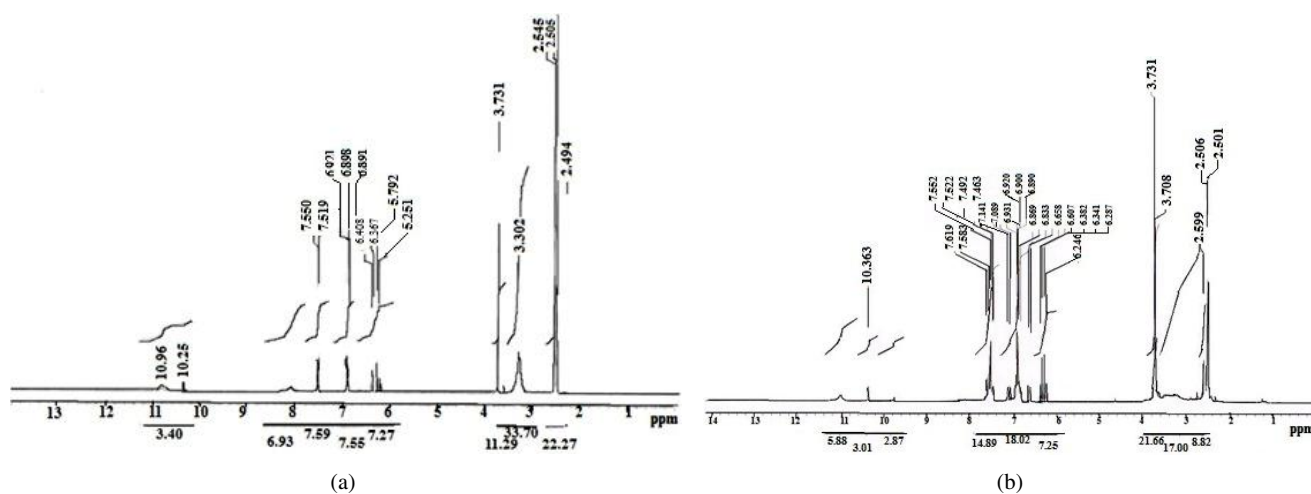


Figure 2: (a) $^1\text{H-NMR}$ spectrum of Mo complex of ML ligand. (b) $^1\text{H-NMR}$ spectrum of W complex of ML ligand.

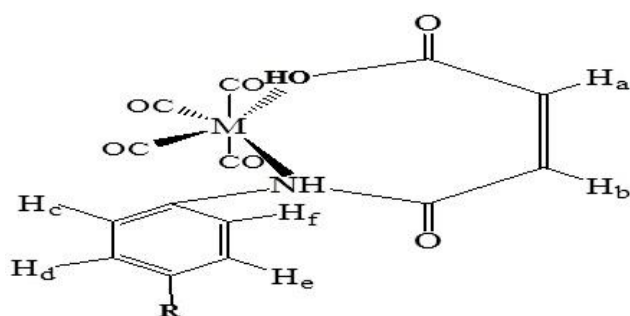


Figure 3: The proposed structure of complexes, $\text{M} = \text{Cr}, \text{Mo}$ or W and $\text{R} = \text{OCH}_3$ or F .

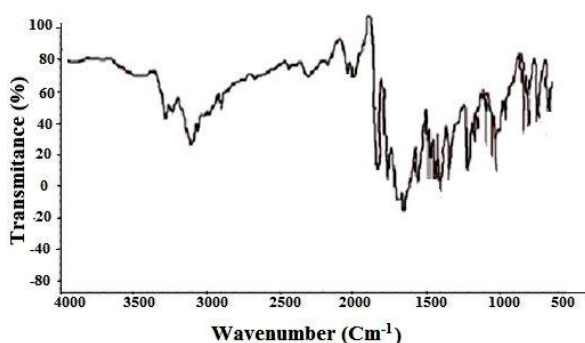


Figure 4: FT-IR spectrum of ML ligand.

On the other hand, the spectra of ML ligand complexes 2–3 of the type $[\text{M}(\text{CO})_4\text{ML}]$ (Figures 2(a) and 2(b)) show a shift in the free ligand carboxylic OH proton signal, confirming the possibility of chelation through OH group of the free ligand carboxylic group. The signal of H-NCO free ligand proton is slightly shifted in the spectra of the metal complexes indicating the possibility of sharing the ML amide group in the coordination process. The doublet

of doublets signals of the ML ligand aromatic protons are slightly shifted in the spectra of its complexes. The free ligand vinylic proton H^a is slightly shifted to δ 6.37–6.25 ppm and δ 6.34–6.24 ppm for Mo and W complexes, respectively. The other vinylic proton H^b is slightly shifted to δ 6.41–6.29 ppm and δ 6.38–6.28 ppm for $[\text{Mo}(\text{CO})_4\text{ML}]$ and $[\text{W}(\text{CO})_4\text{ML}]$, respectively. All $^1\text{H-NMR}$ data are listed in Table 2. The above discussion of the $^1\text{H-NMR}$ spectrum of ML maleanilic acid confirms the proposed structure presented in Figure 3.

3.3. FT-IR spectra

The FT-IR spectrum of ML ligand shows a broadband at $3,262\text{ cm}^{-1}$, which may be attributed to ν (O–H) of carboxylic acid group vibration frequency [22]. The strong stretching band at $1,699\text{ cm}^{-1}$ may be assigned to ν (C=O) of the carboxylic group. The strong bands observed at $3,000\text{ cm}^{-1}$ and $3,068\text{ cm}^{-1}$ may be attributed to the aromatic ν (C–H) [23]. The medium bands observed at $2,841\text{ cm}^{-1}$, $2,834\text{ cm}^{-1}$, $2,837\text{ cm}^{-1}$, and $2,833\text{ cm}^{-1}$ may be assigned to ν (O–CH₃) of the methoxy group [24]. The ν (N–H) amide stretching band is observed at $3,198\text{ cm}^{-1}$ and the stretching frequency band of the amide carbonyl group ν (C=O) is observed at $1,620\text{ cm}^{-1}$ [25,26]; see Figure 4.

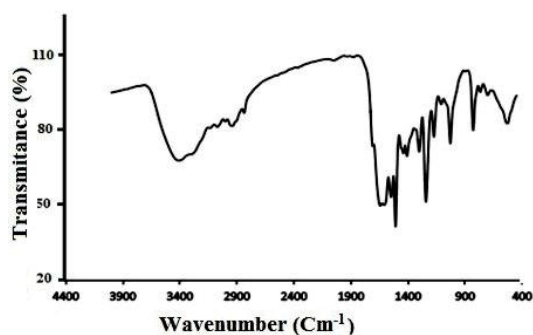
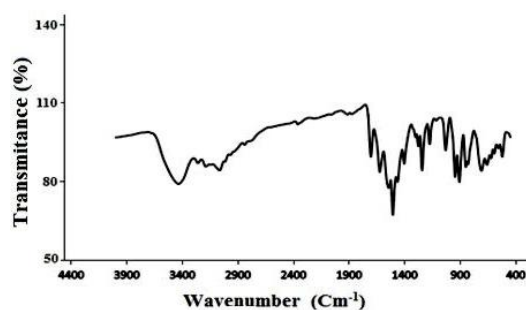
FT-IR frequencies of ML ligand metal complexes are presented in Figures 5–7 and its corresponding data are tabulated in Table 3. The broad ν (O–H) band of the carboxylic acid group of ML ligand is shifted to a higher value in the spectrum of its metal complexes; which means that it is affected by chelation. The strong ν (C=O) stretching band at $1,699\text{ cm}^{-1}$ of the free ligand carboxylic group is shifted to $1,710\text{ cm}^{-1}$, $1,705\text{ cm}^{-1}$, and $1,707\text{ cm}^{-1}$ for $[\text{Cr}(\text{CO})_4\text{ML}]$, $[\text{Mo}(\text{CO})_4\text{ML}]$, and $[\text{W}(\text{CO})_4\text{ML}]$, respectively [22,23,24,27]. The ν (C–O) band of the free ligand carboxylic group

Table 2: $^1\text{H-NMR}$ data of ML, FL ligands and their Mo and W complexes.

Compound	$\delta\text{O-H}$	$\delta\text{N-H}$	$\delta\text{O-CH}_3$	δH^a	δH^b	δH^c	δH^d	δH^e	δH^f	^3J ($\text{H}^a\text{-H}^b$)	^3J ($\text{H}^c\text{-H}^d$)	^3J ($\text{H}^e\text{-H}^f$)
ML	12.88	10.38	3.73	6.42 6.45	6.40 6.43	7.57 7.53	6.93 6.92	6.93 6.92	7.56 7.52	6	3	2.4
FL	11.99	10.35	—	7.23 7.27	7.21 7.25	7.78 7.77	7.48 7.43	7.48 7.43	7.78 7.77	6.3	6.6	1.8
2	10.96	10.25	3.73	6.37 6.25	6.41 6.29	6.91 7.55	6.88 7.52	6.88 7.52	6.91 7.55	12	9	9
3	11.3	10.36	3.73	6.34 6.24	6.38 6.28	6.90 7.52	6.93 7.55	6.93 7.55	6.90 7.52	12	9	9
5	10.82	10.59	—	6.40 6.26	6.44 6.30	7.63 7.13	7.66 7.16	7.66 7.16	7.63 7.13	12	9	9
6	10.66	10.50	—	6.41 6.27	6.45 6.30	7.62 7.13	7.65 7.16	7.65 7.16	7.62 7.13	12	9	9

Table 3: FT-IR spectra of ML, FL free ligands and their complexes 1–6.

Compound	$\nu(\text{C=O})$ (COOH)	$\nu(\text{C=O})$ amide(I) (N-C=O)	$\nu(\text{OH})$	$\nu(\text{C-H})$ aromatic	$\nu(\text{C-O})$ (COOH)	$\nu(\text{NH})$ amide	$\nu(\text{M-O})$	$\nu(\text{C=O})$ carbonyl	$\nu(\text{M-C})$
ML	1,699 s	1,620 m	3,262 s	3,068 w 3,000 w	1,304 m	3,198 w	—	—	—
FL	1,702 s	1,595 m	3,270 s	3,093 w 3,050 w	1,320 m	3,209 w	—	—	—
$\text{Cr}(\text{CO})_6$	—	—	—	—	—	—	—	2,043 s	600
$\text{Mo}(\text{CO})_6$	—	—	—	—	—	—	—	2,000 s	550
$\text{W}(\text{CO})_6$	—	—	—	—	—	—	—	2,073 s	540
1	1,710 s	1,611 m	3,049	3,073 w 3,020 w	1,243 m	3,409 w	550	2,047-1,935-1,869	527 s
2	1,705 s	1,625 m	3,436	3,067 w 3,010 w	1,243 m	3,436 w	558	2,049-1,914-1,872	521 m
3	1,707 s	1,632 m	3,425	3,063 w 3,017 w	1,241 m	3,429 w	594	2,049-1,918-1,873	520 m
4	1,704 s	1,657 m	3,342	3,072 w 3,092 w	1,217 m	3,294 w	516	2,208-1,953-1,878	542 m
5	1,701 s	1,633 m	3,420	3,067 w 3,016 w	1,221 m	3,255 w	601	2,076-1,903-1,879	487 m
6	1,702 s	1,633 m	3,416	3,066 w 2,970 w	1,219 m	3,250 w	595	2,056-1,901-1,876	485 m

**Figure 5:** FT-IR of ML chromium complex 1 [$\text{Cr}(\text{CO})_4\text{ML}$].**Figure 6:** FT-IR of ML molybdenum complex 2 [$\text{Mo}(\text{CO})_4\text{ML}$].

is shifted to $1,243\text{ cm}^{-1}$, $1,243\text{ cm}^{-1}$, and $1,241\text{ cm}^{-1}$ in the spectra of Cr, Mo, and W complexes, respectively. This

may indicate to the sharing of the free ligand hydroxyl oxygen atom in the coordination process. The aromatic

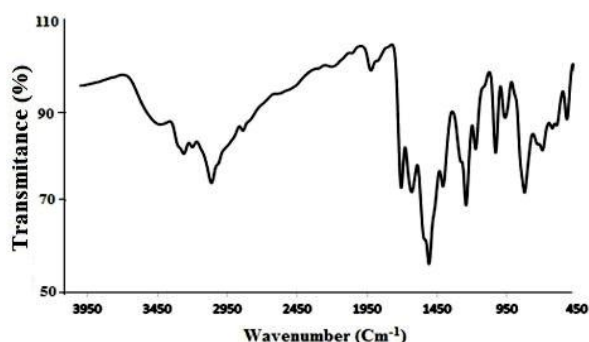


Figure 7: FT-IR of ML tungsten complex 3 [W(CO)₄ML].

ν (C–H) strong bands of the ML ligand are slightly shifted to (3,073 cm⁻¹, 3,020 cm⁻¹), (3,067 cm⁻¹, 3,010 cm⁻¹), and (3,063 cm⁻¹, 3,017 cm⁻¹) in the spectra of Cr, Mo, and W complexes, respectively. The medium bands of the methoxy group ν (O–CH₃) are observed at 2,834 cm⁻¹, 2,837 cm⁻¹, and 2,833 cm⁻¹ in the spectra of [Cr(CO)₄ML], [Mo(CO)₄ML], and [W(CO)₄ML], respectively [23]. The ν (N–H) amide stretching band of the ML ligand is shifted by 200–240 cm⁻¹ in the spectra of [Cr(CO)₄ML], [Mo(CO)₄ML], and [W(CO)₄ML], respectively. This result may indicate the coordination of the free ligand upon the nitrogen of the amide group [23]. The stretching frequency band of the amide carbonyl group ν (C=O) is shifted to 1,611 cm⁻¹, 1,625 cm⁻¹, and 1,632 cm⁻¹ in the spectrum of its complexes, despite of the fact that this (C=O) group does not participate in the coordination. This shift in frequency is a common feature for the amide which coordinates through its nitrogen atom [28]. The ν (N–H) deformation band of ML free ligand observed at 761 cm⁻¹ is slightly shifted in the spectrum of its metal complexes. This confirms the coordination of ML ligand with the metal atoms [29]. The strong bands at 2,043 cm⁻¹, 2,000 cm⁻¹, and 2,073 cm⁻¹ in the spectra of Cr(CO)₆, Mo(CO)₆, and W(CO)₆ may be attributed to ν (CO) of the four-terminal carbonyl groups [30,31]. The metal chelates of carbonyl groups are observed as three stretching bands. One stretching band is observed at (2,047, 2,049, and 2,047) cm⁻¹; which may be assigned to the two symmetrical carbonyl groups in the metal chelates. The other two stretching bands are observed at (1,869, 1,872, and 1,873) cm⁻¹ and (1,919, 1,908, and 1,918) cm⁻¹ may be attributed to the remaining two CO groups; one as symmetrical ν_{sym} (CO) and another as asymmetrical ν_{asym} (CO) for Cr, Mo, and W complexes, respectively [30]. The coordination has also been proved from the appearance of stretching bands corresponding to ν (M–O) and ν (M–N) in the FT-IR spectra of ML complexes [32]. The ν (C–M) stretching frequency of (M–CO) bond of hexacarbonyl metals Cr(CO)₆, Mo(CO)₆, and W(CO)₆ is shifted from 441 cm⁻¹, 368 cm⁻¹, and 374 cm⁻¹ [33] to 527 cm⁻¹, 521 cm⁻¹, and 520 cm⁻¹ in the

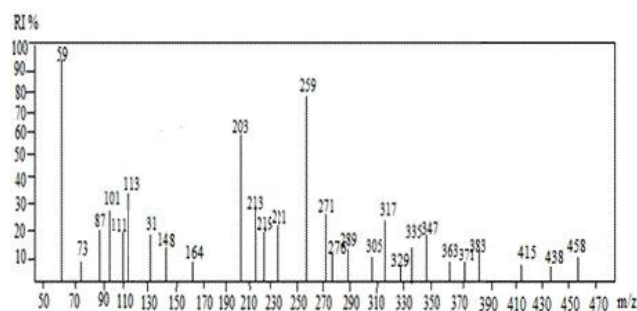


Figure 8: EI-MS of complex 1.

spectra of [Cr(CO)₄ML], [Mo(CO)₄ML], and [W(CO)₄ML] metal complexes, respectively [34].

3.4. EI-MS measurements

The mass spectra of all metal complexes are generally similar. The mass spectrum of chromium complex 1 (Figure 8) is characterized by many competitive and consecutive pathways, forming the main molecular ion and many fragment ions. The fragments are shown in Scheme 2. The signal of moderate intensity (RI = 15%) at $m/z = 383.3$ (M⁺) may be attributed to the molecular ion of [CrC₁₅H₉O₈N]⁺ (mole mass = 384). The fragment ion is fragmented through four parallel pathways. Pathway I shows a fragment ion at $m/z = 163$ (mole mass = 164, RI = 10%); this signal may refer to the rupture of ML maleanilic acid. Pathway II shows fragment ions CrC₁₃H₁₁O₆N⁺, CrC₆H₃O₅N⁺, and CrC₂O₂⁺. These fragment ions are observed at $m/z = 329$, 119, and 111; they may be assigned to the loss of two molecules of CO group from the molecular ion followed by separating *p*-methoxybenzene, then the loss of 4-amino-4-oxobut-2-enoic acid. In pathway III, the signal at $m/z = 221$ (mole mass = 221, RI = 40%) may be assigned to the rupture of Cr(CO)₄ from the molecular ion. The peak at $m/z = 113$ (mole mass = 113, RI = 17%) may be assigned to the loss of 4-methoxybenzene. The final pathway shows signals at $m/z = 276$, 219, and 113 (mole masses = 276, 220, and 115 with RI = 15%, 20%, and 20%), respectively.

3.5. Thermal analyses of the novel metal complexes

The thermal behavior of all ML metal complexes and all FL metal complexes is generally similar. The TGA curve (Figure 9) illustrates the thermal decomposition of complex 1 through two main steps of mass losses. The first step occurs within the temperature range of 250–330 °C and at exactly DTG temperature of 330 °C. This step requires an energy 141.557 kJ.mol⁻¹ of estimated mass loss of 41.7% (calcd. 42.7%), which may be attributed to the removal of both *p*-methoxybenzene group of chemical formula C₇H₈O (mole mass = 108 g) and two molecules of CO gas (mole mass = 56 g). The second step occurs within the temperature range 330–450 °C and with a

Table 4: Thermoanalytical results (TG and DTG) of ML, FL complexes 1–6.

Compound	Temp. range (°C)	% Mass loss found (calcd.)	Assignment
1 [Cr(CO) ₄ ML]	250–330	41.7 (42.7)	– The loss of 4-methoxybenzene + 2CO
	330–450	27.92 (29)	– The loss of 4-amino-4-oxobut-2-enoic acid
2 [Mo(CO) ₄ ML]	130–180	22.44 (21.57)	– The loss of OH ₃ C–C ₆ H ₅
	180–435	13.05 (12.18)	– The loss of HO–CH ₂ –CH ₂ –NH ₂
3 [W(CO) ₄ ML]	131–280	34.6 (37.32)	– The loss of ML maleanilic acid ligand
	280–350	4.33 (4.74)	– The loss of CO group
	350–589	4.64 (4.74)	– The loss of CO group
4 [Cr(CO) ₄ FL]	131.9–395.8	32.69 (30)	– The loss of <i>p</i> -fluoroaniline
	399–509	28.65 (26.8)	– The loss of (Z)-4-oxobut-2-enoic acid
5 [Mo(CO) ₄ FL]	140.7–233.3	2.9 (3.8)	– The loss of fluorine
	233.3–431.3	37.76 (38.78)	– The loss of maleanilic acid ligand
6 [W(CO) ₄ FL]	141–336	16.83 (17.81)	– The loss of <i>p</i> -fluoroaniline
	337–598	12.27 (9.88)	– The loss of (Z)-4-oxobut-2-enoic acid

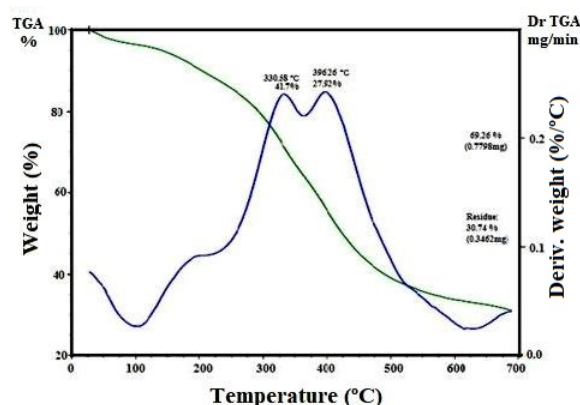
Table 5: Kinetic and thermodynamic parameters data of the metal complexes 1–6.

Compound	Step	Temp. range (°C)	E* (kJ.mol ⁻¹)	A (S ⁻¹)	ΔS* (JK ⁻¹ .mol ⁻¹)	ΔH* (kJ.mol ⁻¹)	ΔG* (kJ.mol ⁻¹)
1 [Cr(CO) ₄ ML]	1	250–330	141.557	1.23442E+12	–234.19	136.534	277.887
	2	330–450	116.684	132830241.1	–236.66	111.116	269.50
2 [Mo(CO) ₄ ML]	1	130–180	197.467	1.40428E+23	–228.69	193.851	293.261
	2	180–435	20.874	759103782.8	–251.44	14.976	193.222
3 [W(CO) ₄ ML]	1	131–280	64.90	8.455E+05	–134.95	61.13	122.26
	2	282–350	135.13	1.807E+11	–33.86	130.89	148.13
	3	350–589	46.73	5.413E+07	–103.04	41.53	105.93
4 [Cr(CO) ₄ FL]	1	131–395	31.00	5.670E+07	–99.41	27.48	69.54
	2	399–509	158.93	3.689E+10	–49.59	153.20	187.36
5 [Mo(CO) ₄ FL]	1	140–233	132.64	1.429E+14	22.42	128.78	118.41
	2	233–431	49.61	2.622E+06	–127.49	44.84	117.89
6 [W(CO) ₄ FL]	1	141–336	43.5	1.950E+06	–129.65	38.9	110.6
	2	338–598	43.89	4.671E+07	–104.55	38.50	106.21

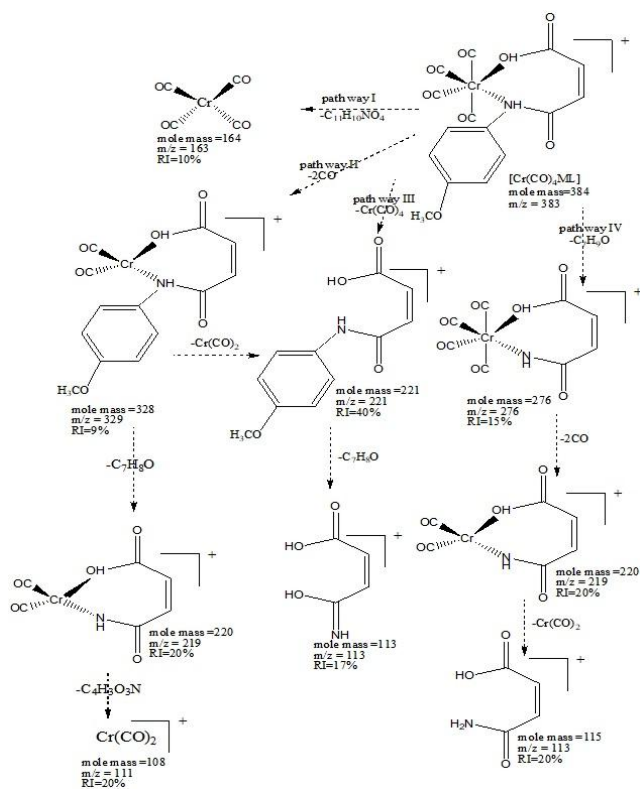
DTG peak at 396 °C. This step requires an energy of 116.68 kJ.mol⁻¹ and it may refer to the estimated mass loss of 27.92% (calcd. 29%), which may be attributed to the loss of 4-amino-4-oxobut-2-enoic acid (mole mass = 115 g). The total mass loss may be 69.26% (calcd. 71.7%) and the remainder may be Cr(CO)₂ of estimated mass loss of 30.38% (calcd. 28.3%). These data are tabulated in Table 4. The values of the obtained thermodynamic parameters are E* (141.557 and 116.684 kJ.mol⁻¹), ΔS* (–234.19 and –236.66 JK⁻¹.mol⁻¹), ΔH* (136.534 and 111.116 kJ.mol⁻¹), and ΔG* (277.887 and 269.50 kJ.mol⁻¹); see Table 5. The thermal behavior of the other metal complexes is presented in Tables 4 and 5.

3.6. The correlation between the mass spectrum and the thermal analyses of the metal chelates

The mass spectrum of [Cr(CO)₄ML] (Scheme 2, pathway II) shows that the molecular ion of the metal chelate is observed at m/z = 383.3 (mole mass = 384). This parent ion is exposed to consecutive fragmentations CrC₁₃H₁₁O₆N⁺, CrC₆H₃O₅N⁺, and CrC₂O₂⁺, respectively. These fragment

**Figure 9:** Thermal TGA and DTGA curves of complex 1.

ions are observed at m/z = 329, 119, and 108, respectively. They may be assigned to the loss of two molecules of CO groups from the molecular ion followed by separating *p*-methoxybenzene, then the loss of 4-amino-4-oxobut-2-enoic acid. This possibility of fragmentation is confirmed by the thermal decomposition of the metal chelate. The



Scheme 2: Suggested mass fragmentation of complex 1.

TGA and DTGA thermogram (Figure 9) shows that $[\text{Cr}(\text{CO})_4\text{ML}]$ is decomposed through two steps. The first step occurs within the temperature range 250–330 °C of mass loss = 41.7% (calcd. 42.7%), which may be attributed to the removal of both *p*-methoxybenzene compound and two molecules of CO gas. The second step occurs in the temperature range of 330–396 °C; it may refer to the loss of 4-amino-4-oxobut-2-enoic acid. The total mass loss may be 69.26% (calcd. 71.7%) and the remainder may be $\text{Cr}(\text{CO})_2$ of an estimated mass loss of 30.38% (calcd. 28.3%).

3.7. Biological activity of FL and its chromium complex

Evaluation of the efficacy of FL free ligand as an inhibitor revealed a higher potency against HepG-2, MCF-7, and HCT-116 human cancer cell lines; as shown in Figure 10. The calculated IC_{50} values are $56.2 \mu\text{g mL}^{-1}$, $60.4 \mu\text{g mL}^{-1}$, and $53.7 \mu\text{g mL}^{-1}$ for HepG-2, MCF-7, and HCT-116 cell lines, respectively; as shown in Table 6. The cytotoxic activity of $[\text{Cr}(\text{CO})_4\text{FL}]$ was assayed using HepG-2, MCF-7, and HCT-116 cell lines; the cell viability (%) obtained with continuous exposure for 24 h is depicted in Figure 11.

The IC_{50} values were estimated from the respective dose-response curve and are summarized in Table 6. The resulted data obtained from the cytotoxic activity assay of $[\text{Cr}(\text{CO})_4\text{FL}]$ illustrated that the inhibitory potency of the FL free ligand was obviously weakened when complexed with $\text{Cr}(\text{CO})_6$.

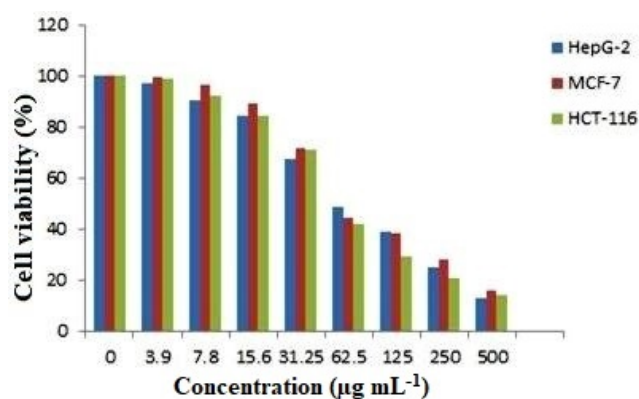


Figure 10: Cell viability of FL against the three tested cell lines.

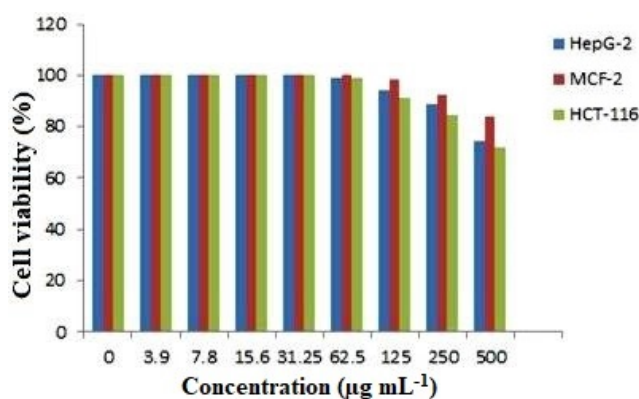


Figure 11: Cell viability of FL chromium complex 3 against the three tested cell lines.

Table 6: Influence of FL and its chromium complex on the viability of tested cell lines.

Compound	In vitro Cytotoxicity IC_{50} ($\mu\text{g mL}^{-1}$)		
	HepG-2	MCF-7	HCT-116
FL	60.4	56.2	53.7
maleanilic acid			
3	>500	>500	>500
$[\text{Cr}(\text{CO})_4\text{FL}]$			

4. Conclusion

ML and FL maleanilic acid derivatives were successfully prepared by crunching the mixture powders of maleic anhydride and different aniline derivatives using an agate mortar at room temperature in a good yield. Elemental analyses, FT-IR, and $^1\text{H-NMR}$ results confirm the proposed structures of these compounds. Also, they prove the success of the synthetic method of these compounds. The synthesized ML and FL ligands coordinate in a molar ratio 1:1 with some transition metals in the form of hexacarbonyl metals $\text{M}(\text{CO})_6$ (where $\text{M} = \text{Cr}, \text{Mo}$ or W). The structure of the novel complexes was confirmed by elemental analyses,

FT-IR, ¹H-NMR, EI-MS, and thermal analyses. These analytical tools confirm that the maleanilic acid derivatives ligands have succeeded in replacing of two carbonyl groups from the hexacarbonyl metals. Furthermore, they prove that the metal carbonyl complexes are in a good agreement with their proposed structures of [M(CO)₄L] in which M = Cr, Mo or W and L = ML or FL maleanilic acid derivatives. The antitumor activities (in vitro) of FL maleanilic acid derivative and its chromium complex against three types of cancer cells [HepG-2, MCF-7, and HCT-116] are studied. It is found that FL free ligand has more antitoxic activity than that of its chromium complex.

Acknowledgments The authors thank the Chemistry Department at Aswan University, the Chemistry Department at Cairo University, and also the staff of the Microanalytical Centre of Cairo University at which all analyses were made.

Conflict of interest The authors declare that they have no conflict of interest.

References

- [1] W. Hieber, *Metal carbonyls, forty years of research*, Adv Organomet Chem, 8 (1970), 1–28.
- [2] C. Elschenbroich, *Organometallics*, Wiley-VCH, Weinheim, 3rd ed., 2006.
- [3] L. B. Epstein and F. Stohlman Jr., *RNA synthesis in cultures of normal human peripheral blood*, Blood, 24 (1964), 69–75.
- [4] M. Siegel and D. Pressman, *The reactions of antiserum homologous to the p-azomaleanilate and p-azofumarinate ion groups*, J Am Chem Soc, 76 (1954), 2863–2866.
- [5] Y. Himeno, T. Hotatsu, K. Arisawa, S. Koshimura, and R. Hirata, *Fundamental studies in chemotherapy of tuberculosis: Part 49. Tuberculo-bacteriostatic experiments with o-aminophenol N-acyl derivatives, and other compounds*, Annu Rep Res Inst Tuberc Kanazawa Univ, 12 (1954), 5–8.
- [6] B. Ramamurthy, G. Ramananda Rao, R. K. Maller, T. Ramakrishnan, and M. V. Bhatt, *N-[2-naphthyl] glycine hydrazide—A potent inhibitor of Mycobacterium tuberculosis H₃₇R_v*, J Indian Inst Sci, 60 (1978), 205–213.
- [7] V. Ravindar and P. Lingaiah, *Effect of amide group ligands and their metal complexes on pathogenic fungi*, Curr Sci, 53 (1984), 1032–1034.
- [8] M. A. Zayed, M. El-Desawy, and A. Eladly, *Spectroscopic investigation of para-methyl and para-methoxy maleanilic acids in comparison with thermal analyses and theoretical calculations and evaluation of cytotoxicity against carcinoma cells*, Egypt J Chem, 62 (2019), 1519–1536.
- [9] M. Kovacs, G. Pfeifer, and I. Pragai, *Production and testing of hormone-type compounds promoting fruit set*, in Proceedings of the Second International Symposium on Plant Growth Regulators, Sofia, Bulgaria, October 21–24, 1975, T. Kudrev, I. Ivanova, and E. Karanov, eds., Bulgarian Academy of Sciences, Sofia, 1977, 366–371.
- [10] C. Mentzer, C. Molho, and H. Pacheco, *Relations between chemical structure and inhibition of tropisms in plants*, Bull Soc Chim Biol (Paris), 32 (1950), 572–582.
- [11] R. S. Baichwal, R. M. Baxter, S. I. Kandel, and G. C. Walker, *Antifungal action of salicylanilide. II*, Can J Biochem Physiol, 38 (1960), 245–251.
- [12] H. Tripathy, D. G. Pradhan, B. C. Dash, and G. N. Mahapatra, *Synthesis of some new halogenated N-thiazolyl substituted hydroxy acid amides and their use as possible fungicides*, Agric Biol Chem, 37 (1973), 1375–1383.
- [13] R. L. Dutta and A. K. Sarkar, *A study of metal complexes of carbohydrazide*, J Inorg Nucl Chem, 43 (1981), 2557–2559.
- [14] I. S. Ahuja, R. Sriramulu, and R. Singh, *Complexes of Co(II), Ni(II), Cu(II), Zn(II), Cd(II) & Ag(I) nitrates with nicotinic acid & related ligands*, Indian J Chem, 19A (1980), 909–912.
- [15] H. Sigel and R. B. Martin, *Coordinating properties of the amide bond. Stability and structure of metal ion complexes of peptides and related ligands*, Chem Rev, 82 (1982), 385–426.
- [16] R. C. Aggarwal, N. K. Singh, and R. P. Singh, *Magnetic and spectroscopic studies on N-(picolinamido)salicylaldehyde complexes of some bivalent 3d metal ions*, Inorg Chem, 20 (1981), 2794–2798.
- [17] H. Saedi, *Solvent free preparation of N-substituted maleanilic acid*, Bull Chem Soc Ethiop, 27 (2013), 137–141.
- [18] G. R. Cooper, F. Hassan, B. L. Shaw, and M. Thornton-Pett, *Novel routes to functionalized diphosphine-M(CO)₄ complexes (M = W, Mo, or Cr)*, J Chem Soc Chem Commun, 1985 (1985), 614–616.
- [19] T. Mosmann, *Rapid colorimetric assay for cellular growth and survival: application to proliferation and cytotoxicity assays*, J Immunol Methods, 65 (1983), 55–63.
- [20] S. Gomha, S. Riyadh, E. Mahmoud, and M. Elaasser, *Synthesis and anticancer activities of thiazoles, 1,3-thiazines, and thiazolidine using chitosan-grafted-poly(vinylpyridine) as basic catalyst*, Heterocycles, 91 (2015), 1227–1243.
- [21] R. M. Silverstein and G. C. Bassler, *Spectroscopic Identification of Organic Compounds*, John Wiley and Sons, New York, 1967.
- [22] F. Adar, *Spectroscopy—Solutions for material analysis*, 2016.
- [23] C. L. Sharma, P. K. Jain, and T. K. De, *Preparation and characterisation of some mixed ligand complexes of chromium nitrioltriacetate with amino acids*, J Inorg Nucl Chem, 42 (1980), 1681–1687.
- [24] J.-J. Max and C. Chapados, *Infrared spectroscopy of aqueous carboxylic acids: Comparison between different acids and their salts*, J Phys Chem A, 108 (2004), 3324–3337.
- [25] K. A. A. Al-Assadi, *Synthesis, characterization, X-ray determination and electrochemical studies of new nickel (II) cobalt (II) and chromium (III) complexes containing N-phenyl P-carboxylmaleimide ligands*, Int Res J Nat Sci, 4 (2016), 12–23.
- [26] M. A. Zayed, M. El-desawy, and A. A. Eladly, *Experimental and theoretical spectroscopic studies in relation to molecular structure investigation of para chloro, para fluoro and para nitro maleanilic acids*, Comput Biol Chem, 76 (2018), 338–356.
- [27] E. Pretsch, P. Bühlmann, and M. Badertscher, *Structure Determination of Organic Compounds*, Springer-Verlag, Berlin, 4th ed., 2009.
- [28] C. L. Sharma, S. S. Narvi, and R. S. Arya, *Characterisation of Cu(II), Ni(II), Co(II), Pd(II) and Fe(III) complexes of anilic acids*, Acta Chim Hung, 114 (1983), 349–354.
- [29] S. M. Cakić, G. S. Nikolić, J. V. Stamenković, and S. S. Konstantinović, *Physico-chemical characterization of mixed-ligand complexes of Mn(III) based on the acetylacetonate and maleic acid and its hydroxylamine derivative*, Acta Periodica Technologica, 2005 (2005), 91–98.
- [30] M. Kaushik, A. Singh, and M. Kumar, *The chemistry of group-VIb metal carbonyls*, Eur J Chem, 3 (2012), 367–394.
- [31] P. S. Braterman, *Metal Carbonyl Spectra*, Organometallic Chemistry, Academic Press, New York, 1975.
- [32] J. Bergman and T. Brimert, *Addition of secondary amines to maleamic esters and maleimides*, Acta Chem Scand, 53 (1999), 48–56.
- [33] L. H. Jones, *Vibrational spectra and force constants of the hexacarbonyls of chromium, molybdenum and tungsten*, Spectrochim Acta, 19 (1963), 329–338.
- [34] L. H. Jones, *A resonance interaction valence force field for octahedral M(XY)₆ molecules*, J Mol Spectrosc, 8 (1962), 105–120.